NIH Public Access
Author Manuscript
*Int J Mass Spectrom*. Author manuscript; available in PMC 2014 October 15.

Published in final edited form as:
*Int J Mass Spectrom*. 2013 October 15; 352: 9–18. doi:10.1016/j.ijms.2013.07.015.

# Evaluation of ion mobility-mass spectrometry for determining the isomeric heterogeneity of oligosaccharide-alditols derived from bovine submaxillary mucin

**Hongli Li**[a], **Brad Bendiak**[b], **Kimberly Kaplan**[a], **Eric Davis**[a], **William F. Siems**[a], and **Herbert H. Hill Jr.**[a,*]

[a]Department of Chemistry, Washington State University, Pullman, WA, USA

[b]Department of Cell and Developmental Biology and Program in Structural Biology and Biophysics, University of Colorado, Health Sciences Center, Anschutz Medical Campus, Aurora, CO, USA

## Abstract

Rapid separation and independent analysis of isomeric species are needed for the structural characterization of carbohydrates in glycomics research. Ion mobility-mass spectrometry techniques were used to examine a series of isomeric neutral oligosaccharide-alditols derived from bovine submaxillary mucin. Several analytical techniques were employed: (1) off line separation of the oligosaccharide-alditol mixture by HPLC; (2) direct and rapid evaluation of isomeric heterogeneity of oligosaccharides by electrospray ionization-ion mobility-time of flight mass spectrometry; and (3) mobility-selected $MS^2$ and $MS^3$ to evaluate isomeric mobility peaks by dual gate ion mobility-tandem mass spectrometry. Multiple isomeric ion mobility peaks were observed for the majority of oligosaccharide-alditols, which was achieved on the millisecond time scale after LC separation. Fragmentation spectra obtained from the collision-induced dissociation of isomeric precursor ions could be essentially identical, or dramatically different for a given precursor *m/z* using the dual-gate ion mobility quadrupole ion trap mass spectrometer. This further confirmed the need for rapid physical resolution of isomeric precursor species prior to their tandem mass spectral analysis.

### Keywords

Ion mobility-mass spectrometry; Isomeric heterogeneity; Oligosaccharide-alditol; Mobility selected fragmentation; Bovine submaxillary mucin

## 1. Introduction

Carbohydrate isomers result from different stereochemical configurations of the hydroxyl groups at each carbon in their sugar rings, different linkage positions, or/and different numbers of branching points [1–3]. Isomers are ubiquitously present and are usually seen in biological glycan samples [4–6]. Glycans coordinate with glycosyltransferase expression and carbohydrate isomers are frequently related through common core structures in some cases [7–9]. Their analysis still faces a central and nontrivial problem: how to identify and

© 2013 Elsevier B.V. All rights reserved.

*Corresponding author. Tel.: +1 509 335 5648. hhhill@wsu.edu (H.H. Hill Jr.).

**Appendix A. Supplementary data**

Supplementary data associated with this article can be found, in the online version, at http://dx.doi.org/10.1016/j.ijms.2013.07.015.

NIH-PA Author Manuscript
NIH-PA Author Manuscript
NIH-PA Author Manuscript

NIH-PA Author Manuscript

NIH-PA Author Manuscript

NIH-PA Author Manuscript

quantitate the number of species starting from a complex mixture of molecules either known or suspected of being comprised of sets of isomers. Separation of carbohydrate isomers is vitally important both for their structural elucidation and ultimately for understanding the roles these molecules play in biological systems.

One common analytical approach used is MS [10–13]. However, frequently many sets of isomers in carbohydrate samples derived from natural sources can be difficult to assess by MS alone, particularly in cases where precursor ions generate product ions all having the same *m/z*, even after higher stages of tandem mass analysis ($MS^n$). Liquid chromatography (LC) [14–16] has been used to separate complex glycan mixtures prior to MS, but this alone is not effective for detecting similar isomers that co-migrate. Many types of LC separations have been utilized, including normal-phase, ligand-exchange, combined normal-phase ligand exchange, reversed-phase, anion exchange at high pH, gel permeation, and porous graphite columns [4,17–22]. As none of these separations has infinite resolution, isomers are frequently found to co-migrate hence a second column that separates according to some different physical property is then required to evaluate fractions. This requires that multiple fractions be concentrated and then chromatographed a second time, which can be time consuming. Furthermore, there is no guarantee that two columns are adequate for resolving all isomers, in which case the process needs to be repeated using a third column (and the time magnified with even more fractions) to evaluate isomeric heterogeneity. If isomeric precursor ions yield identical product ions, knowledge of whether or not they are present in a mixture is easy to miss. NMR [23–25] typically requires glycans to be in a purified state for structure characterization, which is not easily achievable for biological samples with large numbers of isomeric mixtures. High resolution separation techniques that can rapidly assess a wide variety of separation conditions that resolve isomeric structures are needed.

Ion mobility spectrometry (IMS), separating ions based on their ion-neutral collision cross sections, serves as a robust and fast gas phase separation technique in many fields [26–29] including glycomics research [5,6,30–32]. It has been demonstrated that IMS can resolve many monosaccharide methyl glycoside isomers with subtle structural differences [33,34] and is also capable of distinguishing various oligosaccharide isomers [35–37]. Moreover, with the establishment of a dual gate ion mobility-tandem MS system [38–40], mobility selected fragmentation experiments are now feasible, providing evidence for multiple isomeric precursors as mobility-separated species. A number of studies of carbohydrate isomerism using ion mobility-mass spectrometry (IMMS) in the literature have been performed on purified or commercially available standards [33–40]. With the application of IMMS to biological samples, isomeric ion mobility peaks have been observed [5,6,41]. However, fragmentation patterns for the individual resolved isomeric mobility peaks were rarely reported [6]. Yet this information is critical in assessing the isomeric composition of carbohydrates within a set of mobility-selected peaks at a given *m/z* value.

Here we use neutral oligosaccharide-alditols derived from bovine submaxillary mucin (BSM) as an example to demonstrate the value of IMMS techniques to evaluate the isomeric heterogeneity of precursor ions having selected *m/z* values. BSM neutral O-linked oligosaccharides were chosen because they have been shown to contain a large number of isomers, which posed a challenge to multi-step LC/MS or LC/MS/MS analysis [4]. Ambient pressure IMS coupled to mass spectrometry and tandem mass spectrometry were found to provide advantages for structural glycomics described herein. As the upfront IMS separation can be performed rapidly (millisecond time frame) and subsequent $MS^n$ analysis can still be performed on precursor ions, IMMS gives added value to classical $MS^n$ analyses of isolated *m/z* values.

NIH-PA Author Manuscript

NIH-PA Author Manuscript

NIH-PA Author Manuscript

## 2. Experimental

### 2.1. Chemicals and samples

BSM, $NaBH_4$ and NaCl were purchased from Sigma–Aldrich (St. Louis, MO). All solvents (methanol and water) used were HPLC grade and supplied from J.T. Baker Inc. (Philipsburg, NJ, USA). A mixture of equal volume methanol and water was used as an electrospray ionization (ESI) solvent. Martensson et al. [4] described the procedure for the preparation and separation of neutral oligosaccharide-alditols from BSM, but the procedure was scaled down 10-fold in this preparation. Briefly, 1.0 g BSM was treated with 0.05 M NaOH/1.0 M $NaBH_4$ to release acidic and neutral oligosaccharide-alditols (only the neutral oligosaccharides were used in current study). The neutral oligosaccharide-alditol mixture was concentrated to dryness and then re-dissolved in 10 mL $CH_3CN/H_2O$ (74:26), and injected in 0.5-mL batches onto a semipreparative Glycopak N [42] normal-phase chromatography column (Millipore Corp., Bedford, MA). The column was operated using acetonitrile/water in the range of 85/15–70/30 as a mobile phase at a flow rate of 5.0 mL/min. A set of fractions were collected based on UV absorbance at 200 nm. 10 fractions were collected and rotary evaporated to dryness. Each fraction contains several oligosaccharide-alditols including isomers.

ESI solvent (1 mL) was added to each fraction to prepare stock solutions. Different dilution ratios were used for the different fractions, resulting in final solutions with a concentration of ~0.01 mg/mL for ion mobility-time of flight MS and ~0.1 mg/mL for ion mobility quadrupole ion trap mass spectrometer. Sodiated adducts were exclusively observed for all the oligosaccharide-alditol species in this study. To enhance their formation, either 2 or 10 μL of a 5 mM NaCl solution was added to each 1 mL sample to give a final concentration of 10 μM NaCl for ion mobility-time of flight MS and 50 μM NaCl for ion mobility-quadrupole ion trap MS, respectively.

### 2.2. Ambient pressure resistive glass drift tube ion mobility time of flight mass spectrometer

The instrument was fully described previously by Kaplan et al. in 2010 [43] and will be simply referred as IM-TOFMS in the following text. Voltages used in this study were: 12.5 kV for ESI, 9.0 kV on the entrance of the resistive glass IMS tube, 7300 V on the ion gate and 795 V on the end of the IMS, resulting in a homogeneous electric field of 325 V/cm. A gate pulse width of 0.1 ms was utilized in order to obtain higher resolving power and better evaluate isomeric mixtures. Nitrogen was used as the drift gas at a flow rate of 1.5 L/min.

TofDaqViewer software (TOFWERKS AG) was used to collect all the data from IM-TOFMS. The data from each sample could either be completely or selectively exported based on the user-specified time range in the format of a 2-dimensional (2D) text file. IDL virtual machine software (www.exelisvis.com) was then used to generate 2D IMMS correlation spectra based on the exported text file data.

### 2.3. Ambient pressure dual gate ion mobility quadrupole ion trap mass spectrometer (IM-QITMS)

The system was reported by Clowers et al. [38] previously in detail and has been applied to several studies [40,44]. The voltages applied were as follows: 13 kV for the ESI, 10 kV on the first ring of the IMS, 9.28 and 1.28 kV for the first and second gates of the IMS and 342 V on the last ring. The IMS system was coupled to an LCQ Deca QITMS (Thermo Electron, San Jose, CA) through the extended post-drift region. Nitrogen drift gas was introduced at the low-voltage end of the drift tube at a flow rate of 1 L/min. With both gates open, the instrument serves as a quadrupole ion trap mass spectrometer. The two gate ion mobility

NIH-PA Author Manuscript

NIH-PA Author Manuscript

NIH-PA Author Manuscript

control software was rewritten using the Labview 2009 version instead of Labview 6.1 reported previously [38]. There are two operation modes basically [38,40,44]: selected mobility monitoring (SMM) mode which allows a specific drift time window of ions to be transmitted to the ion trap and dual gate scanning mode (DGS) which determines ions' drift times through a successive series of stepped ion gate pulsing experiments. However, the DGS mode is a rather slow process for overall mobility range scanning particularly for complicated samples. Mobility-selected fragmentation was performed in the SMM mode using the $MS^n$ function in the quadrupole ion trap with appropriate timing of gates. The gate pulse width of the first gate was at 0.3 ms for all the SMM experiments in this study. For adjacent peaks, a drift time window of the second gate was selected within the range of 0.2 or 0.3 ms of the central drift time determined on the valley side and was at the corresponding peak edge on the baseline side. The mobility selected $MS^2$ data was acquired for 10 min and $MS^3$ spectrum was collected for 15 min on the IM-QITMS in this study.

### 2.4. Electrospray ionization (ESI) source

All samples were introduced and ionized by ESI in the positive mode. The ESI emitter was prepared in-house using 360 μm o.d. × 100 μm i.d. silica capillary tube (Polymicro Technologies, Phoenix, AZ, USA). It (~5 cm) was connected to the sample transfer line (~15 cm) through a zero dead volume stainless steel union (Valco Instruments Co. Inc., Houston, TX) where ESI voltage was applied. The end of the capillary tube from the ESI emitter was positioned at the center of the IMS tube for IM-TOFMS and with an upward angle of 45° for the IM-QITMS. Samples were injected at a flow rate of 5 μL/min by a Chemyx syringe pump model 200 (Chemyx Inc., Stafford, TX) or an on-board syringe pump.

### 2.5. IMS theory

IMS has been discussed in detail elsewhere [26–29,45]. It is a gas phase separation technique based on the drift velocity of ions ($\boldsymbol{\nu}_d$, cm/s) under a homogeneous electric field ($E$, V/cm) in a counter flow of neutral drift gas. The relationship is expressed by Eq. (1), where $K$ [in $cm^2/(V \times S)$] is termed the mobility coefficient and is related to measureable parameters of the instrument through the following equation,

$$K = \frac{\boldsymbol{\nu}_d}{E} = \frac{L^2}{t_d V} \quad (1)$$

where $L$ is the drift tube length in cm, $V$ is the voltage applied across the drift region in Volts, and $t_d$ is the drift time in seconds. $K$ can be standardized by temperature $T$ (Kelvin) and pressure $P$ (Torr) to a reduced mobility parameter $K_0$ based on Eq. (2)

$$K_0 = \frac{L^2}{t_d V} \times \frac{273.15}{T} \times \frac{P}{760} \quad (2)$$

The two IMMS instruments in this study were operated under the low-field limit. In addition, they were located in the same laboratory (Pullman, WA) and both kept at 200 °C. The drift tube length and voltage applied through the drift region on the IM-QITMS instrument were different from that of the IM-TOFMS, which results in different drift time values for the same compound between the two instruments. However, $K_0$ values are constant for a given compound in a given buffer gas at one temperature. Thus, the drift times of oligosaccharide-alditols on the IM-QITMS instrument were determined using Eq. (2) based on the values obtained from the IM-TOFMS in this study. As defined by the parameters presented above (see Sections 2.2 and 2.3), the relation of $t_{d(\text{IM-QIT})} = 1.32 \times t_{d(\text{IM-TOF})}$ was derived (see Supporting Information), and this was validated by the

NIH-PA Author Manuscript

NIH-PA Author Manuscript

NIH-PA Author Manuscript

instrumental standard 2,6-di-tert-butylpyridine and disaccharide-alditol standard α-d-GalNAc-(1–3)-GalNAc-ol (see Supporting Information).

## 3. Results and discussion

### 3.1. Fractionation of neutral oligosaccharide-alditols and evaluation of their mass-to-charge constituents by LC–MS

In this study, a semi-preparative column, Glycopak N, was used as it has been shown to resolve neutral oligosaccharide isomers as confirmed by MS/MS and $^{1}$H NMR [4]. The HPLC elution profile of a neutral oligosaccharide-alditol mixture from BSM with UV detection at 200 nm is shown in Fig. 1a, where the separation took place in ~4 h. Mass spectra of the entire starting mixture and individual HPLC fractions acquired on the QITMS are displayed in Fig. 1b. In total, 10 fractions were obtained through the collection of peaks and shoulders shown in Fig. 1a that are known to contain isomeric oligosaccharide-alditols [4]. Fraction 1 was not examined as it is virtually entirely the reduced monosaccharide-alditol d-GalNAc-ol as shown by NMR [4]. It is worth pointing out that the early fractions had more sample, with the latter fractions having progressively less from fraction to fraction. Ions of *m/z* 449, 554, 611, 652, 757, 773, 814, 919, 960 and 1065 were the major ions observed and were distributed in different LC fractions, with a general progression from smaller structures in initial fractions to larger structures in later fractions. All the *m/z* values in this paper were attributable to sodium adducts of the oligosaccharide-alditols. LC fractionation followed by concentration of fractions increased the concentration of low abundance *m/z* species which enabled many of them to be studied that were not feasible with the entire mixture, particularly in the later fractions that have less overall abundance. Ions having *m/z* 449 and 554 were mainly observed in fractions 2 and 3, respectively; those at *m/z* 611 and 652 were mainly found in fractions 4–7; those at *m/z* 757 were found in fractions 5–7; those at *m/z* 773 were present in fractions 6–8; those at *m/z* 919 and *m/z* 960 mainly appeared in fractions 8–10; and those at *m/z* 1065 were found in fractions 9 and 10.

Three points are worthy of note regarding oligosaccharide-alditol mixtures as complex as these. First, in collecting peaks largely from valley to valley as shown in Fig. 1a, it is feasible that some structures may be found solely within one peak but some may span parts of both peaks because the valleys do not always come down to baseline. Therefore the same actual compound can be (and sometimes [4] is) found within adjacent peaks. Second, isomers having the same *m/z* can be found in one or more LC peaks (Fig. 1b and [4]). Third, some isomers dissociate to yield identical product ions, sometimes in very similar ratios. For example, we know from previous studies that there are 5 isomers in this sample that have a *m/z* of 449 (d-GlcNAc-β-1-3-d-GalNAc-ol, d-GalNAc-α-1-3-d-GalNAc-ol, d-GalNAc-β-1-3-d-GalNAc-ol, d-GlcNAc-β-1-6-d-GalNAc-ol, and d-GalNAc-α-1-6-d-GalNAc-ol) [4]. The first three dissociate to give the same product ions in nearly equal abundance, as do the latter two. This prompts three questions: (1) How would one know whether different isomers are present in two adjacent LC fractions, as some isomers give identical product ions in nearly the same ratios? (2) How would one know whether the same compound is present in two adjacent LC fractions (i.e. spanning both sides of the valley between fractions), as these dissociation patterns are from the same compound hence would be identical? (3) How would one know whether different isomers are present in the same LC fraction when they give essentially identical dissociation patterns? Clearly, some technique is required such as physical separation of isomers or ion spectroscopy to discriminate species that yield near-identical dissociation spectra.

NIH-PA Author Manuscript

NIH-PA Author Manuscript

NIH-PA Author Manuscript

### 3.2. Rapid evaluation of isomeric heterogeneity of neutral O-linked oligosaccharide-alditols using IM-TOFMS

Individual HPLC fractions were analyzed by IMMS to evaluate whether they could be resolved into two or more isomeric mobility peaks. The complete mixture of oligosaccharide-alditols from BSM and individual HPLC fractions were analyzed using the IM-TOFMS system and data was acquired for 5 min per sample. Unfortunately, for 2D mass-mobility correlation spectra using the entire mixture of oligosaccharide-alditols, only low mass ions were observed with high intensity. Most higher mass ions were found at much lower intensities, which is probably due to (1) overall greater quantities of the lower mass components (2) charge competition and (3) low duty cycle of the IMS (a narrow gate width of 0.1 ms used).

Fig. 2 shows the overlaid 2D mass-mobility correlation spectra and the additional 1D overlaid mobility profiles for selected *m/z* components in different fractions. Since only two 2D spectra can be overlaid at the same time using the IDL software developed for the instrument in this study, in order to compare mobility profiles for a specific *m/z* in multiple LC fractions, additional overlaid 1D mobility spectra are aligned on the right with the same drift time scale as the 2D spectrum. Different fractions are denoted with different colors as labeled for individual plots. For example, Fig. 2a displays the overlaid 2D mass-mobility profiles for *m/z* 611 from fractions 4 (blue) and 5 (black). Shown on the right are overlaid 1D mobility spectra for *m/z* 611 from fractions 5 (black) and 6 (red). It was observed that the *m/z* 611 precursor ions in fractions 4 and 6 had different drift times, hence they are isomers. As studied previously, three isomers of *m/z* 611 were reported with the relative amounts of 4.0:2.2:0.27 [4], thus the minor mobility peak for *m/z* 611 in fraction 5 which had the same drift time as *m/z* 611 from fraction 4 may represent a different minor isomer. The *m/z* 611 ion was a sodium adduct ion with the proposed composition of $Hex_1HexNAc_1HexNAc$-ol. Other examples in Fig. 2 include sodiated trisaccharide-alditols with composition $HexNAc_2HexNAc$-ol at *m/z* 652 (Fig. 2b) from fractions 4, 5 and 6, sodiated tetrasacchride-alditols with composition $DeoxyHex_1Hex_1HexNAc_1HexNAc$-ol at *m/z* 757 from fractions 5, 6 and 7 (Fig. 2c), $Hex_2HexNAc_1HexNAc$-ol at *m/z* 773 from fractions 6, 7 and 8 (Fig. 2d), $Hex_1HexNAc_2HexNAc$-ol at *m/z* 814 from fraction 7 (Fig. 2e); and hexasaccharide-alditol $DeoxyHex_2Hex_2HexNAc_1HexNAc$-ol at *m/z* 1065 (Fig. 2f) from fraction 9. The composition information was validated by the *m/z* values and fragmentation patterns. For fraction 10, the signal accumulated on the IM-TOFMS instrument was extremely low which was primarily due to the relatively small amount of sample gathered from the LC and hence no data is presented here. For each individual plot in Fig. 2, only a narrow *m/z* range is selectively displayed where multiple peaks on the *m/z* axis represent the main ion along with its corresponding (mainly $^{13}C$) isotopomers. It is clear that all the ions have more than one mobility peak detected along the ion mobility (vertical) axis which indicates multiple isomeric forms. Low abundance mobility peaks were confirmed by the reproducibility of multiple runs of the same sample. Colored cross peaks show visually the relative intensities of isomer distributions and their ion mobilities. For low abundance isomers, depending on the intensity threshold selected, cross peaks were sometimes not observable yet could be observed in the 1D mobility plots along the vertical axis for selected *m/z* values.

Overall, 2 isomeric peaks were detected for *m/z* 611, *m/z* 652 and *m/z* 814; 4 different drift time distributions including shoulders were observed for *m/z* 757 and *m/z* 773; 3 partially separated mobility peaks were detected for *m/z* 1065. The results show that (1) IMS can resolve isomeric oligosaccharides in the millisecond time frame that co-migrated in LC peaks, (2) the technique is orthogonal to the physical interactions governing many LC separations and (3) can be performed without any prior knowledge of the nature of isomeric structures or their spectroscopy such as specific UV–vis or IR absorption wavelengths. Of

NIH-PA Author Manuscript

NIH-PA Author Manuscript

NIH-PA Author Manuscript

course, no separation technique has infinite resolving power therefore coincidental co-migration of some compounds, even after HPLC and ion mobility separation, is not unexpected.

### 3.3. Mobility selected fragmentation by dual gate IM-QITMS

While multiple isomers may be observed by IMS how can one confirm or validate the isomeric information obtained by IM-TOFMS? First, oligosaccharide standards might be used to evaluate the ion mobility times. However, in cases where samples are derived from unknown origins or even in cases where they may be known, isolation of the standards for ion mobility comparisons may be time consuming. Moreover, there may not be only one isomeric component in a single ion mobility peak. The conventional method, widely accepted by the mass spectrometry community, is to acquire $MS^n$ spectra of individual isomers that may be used for the confirmation of isomeric species. For multiple isomers having a specific *m/z* found in single LC fractions, ion mobility information combined with mobility selected fragmentation information can be used to discriminate between many isomeric components. It should be pointed out that in Figs. 3–6 the second gate drift time windows used to select isomeric mobility peaks on the IM-QITMS instrument are different from their corresponding drift times acquired on the IM-TOFMS instrument as discussed previously, but they are in agreement with reduced mobility values.

Fig. 3 a displays the 2D IMMS spectra of *m/z* 449 from HPLC fraction 2 with three isomeric mobility peaks labeled. A barely separated shoulder was detected on the side of peak 1 having a longer drift time. By comparing the overlaid individual mobility profiles of available disaccharide-alditol standards isolated from BSM (supporting information), it was found that α-d-GalNAc-(1-3)-d-GalNAc-ol and β-d-GlcNAc-(1-3)-d-GalNAc-ol co-eluted as peak 1, α-d-GalNAc-(1-6)-d-GalNAc-ol co-eluted with the barely separated shoulder of peak 1, peak 2 matched with β-d-GlcNAc-(1-6)-d-GalNAc-ol. The exact structure of the mobility peak (peak 3) with the longest drift time remains unknown but may be the additional structure β-d-GalNAc-(1-3)-d-GalNAc-ol [4] which was not available or possibly another HexNAc-HexNAc-ol, as there were still additional LC peaks reported previously [4] that were not fully characterized. Therefore, in complex mixtures, it is feasible and actually expected that some isomeric forms of oligosaccharides may happen to co-migrate when one specific adduct or gas is used. Fig. 3b and c shows the mobility selected fragmentation spectra for mobility peaks 1 and 2, respectively as labeled in Fig. 3a, by setting the second gate windows at 42.2–43.1 or 44.1–44.6 ms on the dual gate IM-QITMS. They shared the major fragments such as *m/z* 431, *m/z* 389, *m/z* 286 and *m/z* 246, but with different intensity ratios. According to the MS/MS spectra of the available disaccharide-alditol *m/z* 449 standards acquired (supporting information), the fragmentation pattern in Fig. 3c (mobility peak 2) matched with the tandem spectrum of β-d-GlcNAc-1–6-d-GalNAc-ol which was consistent with the data described above, while Fig. 3b (mobility peak 1) was a combination of the spectra of other standards that co-migrated in this mobility window. Additionally, the MS/MS spectrum of isomeric peak 3 was not obtained due to its extremely low intensity.

Fig. 4a shows the 2D mass mobility correlation plot for the ion at *m/z* 757 from HPLC fraction 6, acquired on the IM-TOFMS instrument. Two peaks are labeled on the IMS plot shown along the right vertical axis. In Fig. 4b and c, the tandem spectra are presented for peaks 1 and 2 acquired on the IM-QITMS instrument by setting the second gate drift time windows between 57.4–58.1 and 59.1–60.0 ms, respectively. Since mobility-selected $MS^2$ spectra of the *m/z* 757 ion for isomeric mobility peaks 1 and 2 showed essentially very similar spectra (supporting information), the mobility selected tandem spectra shown here are $MS^3$ spectra of the major product ion *m/z* 611 derived from precursor ion *m/z* 757. Product ions of *m/z* 388, 408, 431, 449, 491, 551 and 593 were observed in both spectra, but

NIH-PA Author Manuscript

NIH-PA Author Manuscript

NIH-PA Author Manuscript

the relative intensities were different. The *m/z* 388 ion was the major product ion for isomeric mobility peak 2, while *m/z* 408 and 449 were of much higher intensity for isomeric mobility peak 1. As illustrated by Zhu et al. [40], *m/z* 757 isomers having the HexNAc-ol substituted at different positions can have either *m/z* 388 or *m/z* 408/449 as the characteristic product ions. The fragmentation pathways for isolated standards were also included in his study [40]. Different tandem spectra obtained in this example validated the isomeric mobility peaks detected and also may provide evidence for potential structure elucidation.

The analysis of isomeric precursor ions of *m/z* 919 (sodium adduct) having the composition of [$DeoxyHex_1Hex_2$ $HexNAc_1$HexNAc-ol] is presented in Fig. 5. Shown in Fig. 5a are the overlaid 2D IMMS spectra of *m/z* 919 in fractions 8 and 9 and in total 3 isomeric mobility peaks labeled as 1, 2 and 3 were detected. Two partially separated isomeric mobility peaks (peaks 2 and 3) were detected for *m/z* 919 in fraction 9 (red trace, Fig. 5a). Note that the barely separated faster mobility shoulder in fraction 8 labeled as mobility peak 1 (black trace, Fig. 5a) indicates another isomeric form for the *m/z* 919 precursor ion. Due to the sensitivity limitation of the instrument and the low resolution between isomeric peaks 1 and 2 in fraction 8, it was not possible to acquire the mobility-separated fragmentation data for *m/z* 919 in fraction 8. Fig. 5b and c display the mobility selected MS/MS spectra of isomeric mobility peaks 2 and 3 of *m/z* 919 in fraction 9 using second gate drift time windows of 65.0–65.8 and 66.4–66.9 ms on the dual gate IM-QITMS, respectively. The two spectra were very similar and both had *m/z* 773 as a predominant product ion through the neutral loss of a DeoxyHex residue. However, a minor difference was observed having *m/z* 593 detected only in Fig. 5b and *m/z* 534 only appeared in Fig. 5c. An additional isolation/dissociation step ($MS^3$) was then further performed for the isomeric peaks 2 and 3 in HPLC fraction 9 using *m/z* 773 as the second-stage precursor ion derived from the *m/z* 919 ion, as shown in Fig. 5d and e. The *m/z* 611 ion derived from the apparent neutral loss of a Hex residue was the major fragment from *m/z* 773 in both spectra. Fragments of *m/z* 388, 408 and 755 were also shared by isomeric mobility peaks 2 and 3. However, there were differences in dissociation of the *m/z* 773 product ion. Fragments of *m/z* 449, 551, 593 and 714 were only found upon dissociation of the *m/z* 773 ion derived from isomeric mobility peak 2 (Fig. 5d), while product ions of *m/z* 422, 557 were uniquely present for the *m/z* 773 ion derived from isomeric mobility peak 3 (Fig. 5e). Moreover, the relative intensities of *m/z* 388 and *m/z* 408 in Fig. 5d and e were different. Further fragmentation of *m/z* 611 might give more structural evidence to differentiate isomeric mobility peaks 2 and 3, but this was beyond the sensitivity capability of the current instrument.

The same criteria were applied to the isomeric pentasaccharide-alditols of $DeoxyHex_1Hex_1HexNAc_2$HexNAc-ol having *m/z* 960 (HPLC fractions 8 and 9) as shown in Fig. 6. Fig. 6a displays the overlaid 2D IMMS spectra of the *m/z* 960 precursor ion from fractions 8 and 9. Four different drift time distributions were observed in all: two isomeric mobility peaks 1 and 3 were observed for *m/z* 960 in fraction 8 and another two isomeric mobility peaks 2 and 4 were detected for *m/z* 960 in fraction 9. In addition, the valley between isomeric mobility peaks 1 and 3 may represent another isomeric form which was overlapped with isomeric mobility peak 2 in fraction 9. Mobility-selected fragmentation was only performed for isomeric mobility peaks 1 and 3 in fraction 8, not for low abundance or barely separated mobility peaks in fraction 9 in this example. Shown in Fig. 6b and c are $MS^2$ spectra of the *m/z* 960 precursor ion corresponding to isomeric peaks 1 and 3 in fraction 8 by selectively transferring them to the QITMS using second gate drift time windows of 66–66.6 and 67.4–68.4 ms, respectively. The spectra are very similar and shared the predominant fragment *m/z* 814 (loss of DeoxyHex from *m/z* 960) and fragments *m/z* 757 (loss of HexNAc from *m/z* 960) and 652 (loss of DeoxyHex-Hex from *m/z* 960) which was consistent with previous structural evidence [4]. Considering the monosaccharide makeup and biosynthetic mechanisms for generating O-linked oligosaccharides, it is not unusual to

NIH-PA Author Manuscript

NIH-PA Author Manuscript

NIH-PA Author Manuscript

observe similar or even identical CID pathways for closely structurally-related oligosaccharide-alditols in BSM [40]. Changing the stereochemistry of one sugar at one position may not have much of an effect on their MS and tandem mass spectra, especially when they fragment in the positive mode where the main fragments frequently result from cleavages at glycosidic bonds. Thus IMS becomes even more relevant and important in the evaluation of the isomeric heterogeneity of oligosaccharides in cases where similar or even identical fragmentation spectra may be obtained. Further fragmentation of isomeric mobility peaks 1 and 3 was carried out to $MS^3$ by selecting *m/z* 814 as the second-stage precursor ion as shown in Fig. 6d and e. Major product ions at *m/z* 611 and 449 were observed for isomers from both ion mobility-selected peaks. However, different fragments were found in each spectrum, for example, *m/z* 754, 635, 593 in Fig. 6d and *m/z* 797, 772, 694, 575, 516, 507 in Fig. 6e. Higher order $MS^n$ of product ions such as *m/z* 611 may be needed in order to further distinguish the structural differences between isomeric peaks 1 and 3. In practice, this is again limited by the sensitivity of the dual gate IMMS instruments and the diminishing amounts of successive product ions available in multi-stage ion trap dissociation experiments.

As shown in above examples, valuable information regarding the isomeric heterogeneity of oligosaccharide-alditols was obtained by combining mobility differentiation and mobility selected $MS^n$ data, which clearly showed that isomers were present for virtually all precursor ions and also demonstrated the advantages of IMMS for exploring the complexity of carbohydrate structures. However, the exact structure(s) for each isomeric mobility peak in this study could not be elucidated since the tandem spectra collected from a single mobility peak could still be potentially attributed to an isomeric mixture of oligosaccharides.

## 4. Conclusions

Using neutral oligosaccharide-alditols isolated from BSM as a model for O-linked glycoprotein structures, it was demonstrated that ion mobility-mass spectrometry has the capability to rapidly evaluate the isomeric heterogeneity of oligosaccharide mixtures without any prior knowledge required. Even after a single HPLC column, isomeric structures that were present in fractions could frequently be resolved as independent peaks using IMMS. This was demonstrated for structures ranging from disaccharide-alditols to hexasaccharide-alditols. Isomeric precursor ions that would normally be grouped into the same *m/z* pool were thereby separated into isolable drift time windows that enabled independent MS/MS spectra and in some cases $MS^3$ spectra to differentiate isomeric structures or isomer pools. While it is still possible that many ion mobility peaks contain isomeric precursors, ion mobility coupled to tandem stages of mass spectrometry enabled different sets of product ions to be assigned to different isomeric precursors within a given *m/z* pool in some cases. This is clearly an advantage in analysis of complex mixtures of glycans derived from biological sources. A single LC column (even more than one LC column) is frequently inadequate to resolve isomeric species present in complex oligosaccharide samples. While $MS^n$ information is valuable for the structure identification of oligosaccharides, it is desirable to resolve as many isomeric species as possible prior to $MS^n$, and it is valuable simply to know how many isomeric precursor ions may be contributing to $MS^n$ spectra. Clearly, more orthogonal analytical separation steps may be needed to fully resolve isomeric species existing in nature, and as many separation steps as possible that can be routinely concatenated for rapid analyses is a sought-after goal.

## Supplementary Material

Refer to Web version on PubMed Central for supplementary material.

NIH-PA Author Manuscript

NIH-PA Author Manuscript

NIH-PA Author Manuscript

## Acknowledgments

This work was supported by the National Institutes of Health with Grant No. 5R33RR020046. Ching Wu at Excellims Inc. was thanked for providing the ion mobility spectra of disaccharide-alditol standards shown in the supporting information. Additional support was from the supply of the LCQ Deca quadrupole ion trap mass spectrometer from Thermo Finnigan.

## References

1. Raman R, Raguram S, Venkataraman G, Paulson JC, Sasisekharan R. Glycomics: an integrated systems approach to structure–function relationships of glycans. Nature Methods. 2005; 2:817–824. [PubMed: 16278650]
2. Hirabayashi J. Oligosaccharide microarrays for glycomics. Trends in Biotechnology. 2003; 21:141–143. [PubMed: 12679056]
3. Mahal LK. Glycomics: towards bioinformatic approaches to understanding glycosylation. Anti-Cancer Agents in Medicinal Chemistry. 2008; 8:37–51. [PubMed: 18220504]
4. Martensson S, Levery SB, Fang TT, Bendiak B. Neutral core oligosaccharides of bovine submaxillary mucin: use of lead tetraacetate in the cold for establishing branch positions. European Journal of Biochemistry. 1998; 258:603–622. [PubMed: 9874229]
5. Plasencia MD, Isailovic D, Merenbloom SI, Mechref Y, Clemmer DE. Resolving and assigning N-linked glycan structural isomers from ovalbumin by IMS-MS. Journal of the American Society for Mass Spectrometry. 2008; 19:1706–1715. [PubMed: 18760624]
6. Williams JP, Grabenauer M, Holland RJ, Carpenter CJ, Wormald MR, Giles K, Harvey DJ, Bateman RH, Scrivens JH, Bowers MT. Characterization of simple isomeric oligosaccharides and the rapid separation of glycan mixtures by ion mobility mass spectrometry. International Journal of Mass Spectrometry. 2010; 298:119–127.
7. Lowe JB, Marth JD. A genetic approach to mammalian glycan function. Annual Review of Biochemistry. 2003; 72:643–691.
8. Varki, A.; Cummings, R.; Esko, J.; Freeze, H.; Hart, G.; Marth, J. Essentials of Glycobiology. New York: Cold Spring Harber Laboratory Press; 1999.
9. Taylor, ME.; Drickamer, K. Introdution to Glycobiology. Oxford and New York: Oxford University Press; 2003.
10. Zaia J. Mass spectrometry and the emerging field of glycomics. Chemistry and Biology. 2008; 15:881–892. [PubMed: 18804025]
11. Morelle W, Michalski JC. The mass spectrometric analysis of glycoproteins and their glycan structures. Current Analytical Chemistry. 2005; 1:29–57.
12. Morelle W, Michalski JC. Glycomics and mass spectrometry. Current Pharmaceutical Design. 2005; 11:2615–2645. [PubMed: 16101462]
13. Reinhold VN, Reinhold BB, Costello CE. Carbohydrate molecular weight profiling sequence linkage, and branching data: ES–MS and CID. Analytical Chemistry. 1995; 67:1772–1784. [PubMed: 9306731]
14. Chu CC, Ninonuevo MR, Clowers BH, Perkins PD, An HJ, Yin H, Killeen K, Miyamoto S, Grimm R, Lebrilla CB. Profile of native N-linked glycan structures from human serum using high performance liquid chromatography on a microfluidic chip and time-of-flight mass spectrometry. Proteomics. 2009; 9:1939–1951. [PubMed: 19288519]
15. Ninonuevo M, An H, Yin H, Killeen K, Grimm R, Ward R, German B, Lebrilla C. Nanoliquid chromatography-mass spectrometry of oligosaccharides employing graphitized carbon chromatography on microchip with a high-accuracy mass analyzer. Electrophoresis. 2005; 26:3641–3649. [PubMed: 16196105]
16. Pabst M, Bondili JS, Stadlmann J, Mach L, Altmann F. Mass + retention time = structure: a strategy for the analysis of N-glycans by carbon LC-ESI-MS and its application to fibrin N-glycans. Analytical Chemistry. 2007; 79:5051–5057. [PubMed: 17539604]
17. Koizumi K, Utamura T, Kubota Y, Hizukuri S. Two high-performance liquid chromatographic columns for analyses of malto-oligosaccharides. Journal of Chromatography. 1987; 409:396–403.

NIH-PA Author Manuscript

NIH-PA Author Manuscript

NIH-PA Author Manuscript


18. Bendiak B, Orr J, Brockhausen I, Vella G, Phoebe C. Separation of neutral reducing oligosaccharides derived from glycoproteins by HPLC on a hydroxylated polymeric support. Analytical Biochemistry. 1988; 175:96–105. [PubMed: 3245581]
19. Van Halbeek H, Breg J, Vliegenthart JFG, Klein A, Lamblin G, Roussel P. Isolation and structural characterization of low-molecular-mass monosialyl oligosaccharides derived from respiratory mucus glycoproteins of a patient suffering from bronchiectasis. European Journal of Biochemistry. 1988; 177:443–460. [PubMed: 3191924]
20. Rajakyla E. Use of reversed-phase chromatography in carbohydrate analysis. Journal of Chromatography. 1986; 353:1–12. [PubMed: 3700511]
21. Hardy MR, Townsend RR. Separation of positional isomers of oligosaccharides and glycopeptides by high-performance anion-exchange chromatography with pulsed amperometric detection. Proceedings of the National Academy of Sciences of the United States of America. 1988; 85:3289–3293. [PubMed: 3368440]
22. Davies MJ, Smith KD, Carruthers RA, Chai W, Lawson AM, Hounsell EF. Use of a porous graphitized carbon column for the high-performance liquid chromatography of oligosaccharide alditols and glycopeptides with subsequent mass spectrometry analysis. Journal of Chromatography. 1993; 646:317–326. [PubMed: 8408434]
23. Jones DMN, Bendiak B. Novel multi-dimensional heteronuclear NMR techniques for the study of $^{13}$C-*O*-acetylated oligosaccharides: expanding the dimensions for carbohydrate structures. Journal of Biomolecular NMR. 1999; 15:157–168. [PubMed: 10605089]
24. Armstrong GS, Mandelshtam VA, Shaka AJ, Bendiak B. Rapid high-resolution four-dimensional NMR spectroscopy using the filter diagonalization method and its advantages for detailed structural elucidation of oligosaccharides. Journal of Magnetic Resonance. 2005; 173:160–168. [PubMed: 15705524]
25. Dua VK, Rao BNN, Wu SS, Dube VE, Bush CA. Characterization of the oligosaccharide alditols from ovarian cyst mucin glycoproteins of blood group A using high pressure liquid chromatography (HPLC) and high field $^{1}$H NMR spectroscopy. Journal of Biological Chemistry. 1986; 261:1599–1608. [PubMed: 3003076]
26. Eiceman, GA.; Karpas, Z. Ion Mobility Spectrometry. second ed.. Boca Raton, FL: CRC Press Taylor and Francis Group; 2005.
27. McLean JA, Ruotolo BH, Gillig KJ, Russell DH. Ion mobility-mass spectrometry: a new paradigm for proteomics. International Journal of Mass Spectrometry. 2005; 240:301–315.
28. Dwivedi P, Wu P, Klopsch SJ, Puzon GJ, Xun L, Hill HH Jr. Metabolic profiling by ion mobility mass spectrometry (IMMS). Metabolomics. 2008; 4:63–80.
29. Kanu AB, Hill HH. Identity confirmation of drugs and explosives in ion mobility spectrometry using a secondary drift gas. Talanta. 2007; 73:692–699. [PubMed: 19073090]
30. Fenn LS, Mclean JA. Biomolecular structural separations by ion mobility-mass spectrometry. Analytical and Bioanalytical Chemistry. 2008; 391:905–909. [PubMed: 18320175]
31. Fenn LS, Mclean JA. Simultaneous glycoproteomics on the basis of structure using ion mobility-mass spectrometry. Molecular BioSystems. 2009; 5:1298–1302. [PubMed: 19823744]
32. Jin L, Barran PE, Deakin JA, Lyon M, Uhrin D. Conformation of glycosaminoglycans by ion mobility mass spectrometry and molecular modeling. Physical Chemistry Chemical Physics. 2005; 7:3464–3471. [PubMed: 16273147]
33. Dwivedi P, Bendiak B, Clowers BH, Hill HH. Rapid resolution of carbohydrate isomers by electrospray ionization ambient pressure ion mobility spectrometry-time-of-flight mass spectrometry (ESI-APIMS-TOFMS). Journal of the American Society for Mass Spectrometry. 2007; 18:1163–1175. [PubMed: 17532226]
34. Li H, Giles K, Bendiak B, Kaplan K, Siems WF, Hill HH. Resolving structural isomers of monosaccharide methyl glycosides using drift tube and traveling wave ion mobility mass spectrometry. Analytical Chemistry. 2012; 84:3231–3239. [PubMed: 22339760]
35. Fenn LS, Mclean JA. Structural resolution of carbohydrate positional and structural isomers based on gas-phase ion mobility-mass spectrometry. Physical Chemistry Chemical Physics. 2011; 13:2196–2205. [PubMed: 21113554]

NIH-PA Author Manuscript

NIH-PA Author Manuscript

NIH-PA Author Manuscript


36. Clowers BH, Dwivedi P, Steiner WE, Hill HH, Bendiak B. Separation of sodiated isobaric disaccharides and trisaccharides using electrospray ionization-atmospheric pressure ion mobility-time of flight mass spectrometry. Journal of the American Society for Mass Spectrometry. 2005; 16:660–669. [PubMed: 15862767]
37. Yamagaki T, Sato A. Isomeric oligosaccharides analyses using negative-ion electrospray ionization ion mobility spectrometry combined with collisioninduced dissociation MS/MS. Analytical Sciences. 2009; 25:985–988. [PubMed: 19667474]
38. Clowers BH, Hill HH Jr. Mass analysis of mobility-selected ion populations using dual gate ion mobility quadrupole ion trap mass spectrometry. Analytical Chemistry. 2005; 77:5877–5885. [PubMed: 16159117]
39. Zucker SM, Lee S, Webber N, Valentine SJ, Reilly JP, Clemmer DE. An ion mobility/ion trap/photodissociation instrument for characterization of ion structure. Journal of the American Society for Mass Spectrometry. 2011; 22:1477–1485. [PubMed: 21953250]
40. Zhu M, Bendiak B, Clowers BH, Hill HH. Ion mobility-mass spectrometry analysis of isomeric carbohydrate precursor ions. Analytical and Bioanalytical Chemistry. 2009; 394:1853–1867. [PubMed: 19562326]
41. Isailovic D, Kurulugama RT, Plasencia MD, Clemmer DE. Profiling of human serum glycans associated with liver cancer and cirrhosis by IMS-MS. Journal of Proteome Research. 2008; 7:1109–1117. [PubMed: 18237112]
42. Bendiak B, Orr J, Brockhausen I, Vella G, Phoebe C. Separation of neutral reducing oligosaccharide derived from glycoproteins by HPLC on a hydroxylated polymeric support. Analytical Biochemistry. 1988; 175:96–105. [PubMed: 3245581]
43. Kaplan K, Graf S, Tanner C, Gonin M, Fuhrer K, Knochenmuss R, Dwivedi P, Hill HH Jr. Resistive glass IM-TOFMS. Analytical Chemistry. 2010; 82:9336–9343. [PubMed: 20964441]
44. Clowers BH, Hill HH Jr. Influence of cation adduction on the separation characteristics of flavonoid diglycoside isomers using dual gate-ion mobility-quadrupole ion trap mass spectrometry. Journal of Mass Spectrometry. 2006; 41:339–351. [PubMed: 16498610]
45. Eiceman GA. Ion-mobility spectrometry as a fast monitor of chemical composition. Trends in Analytical Chemistry. 2002; 21:259–275.

NIH-PA Author Manuscript
NIH-PA Author Manuscript
NIH-PA Author Manuscript



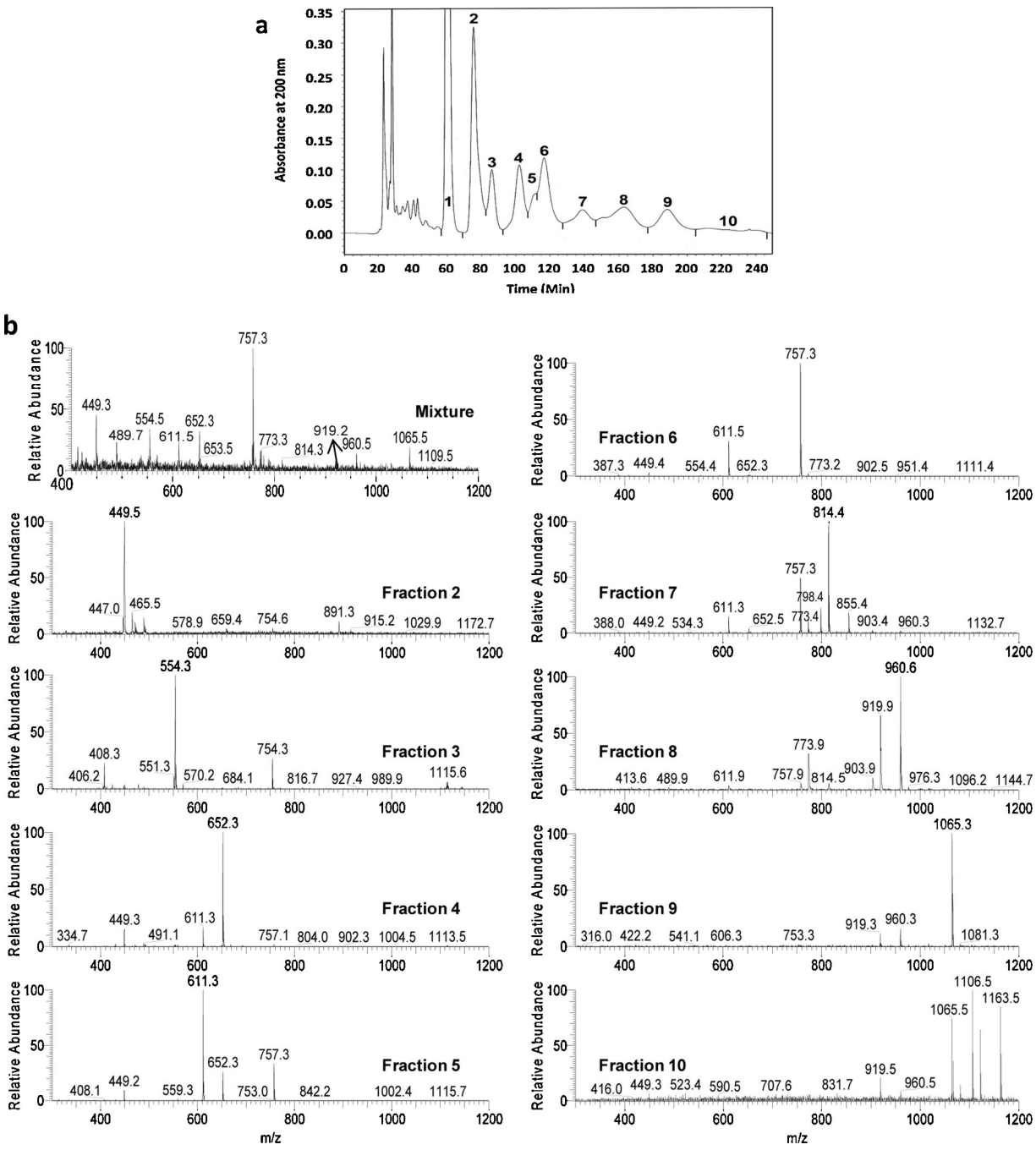


**Fig. 1.**

(a) HPLC elution profile of neutral oligosaccharide-alditols isolated from bovine submaxillary mucin (BSM) and (b) mass spectra of the mixture before separation and of the concentrated individual HPLC fractions 2–10 from panel a.

NIH-PA Author Manuscript
NIH-PA Author Manuscript
NIH-PA Author Manuscript



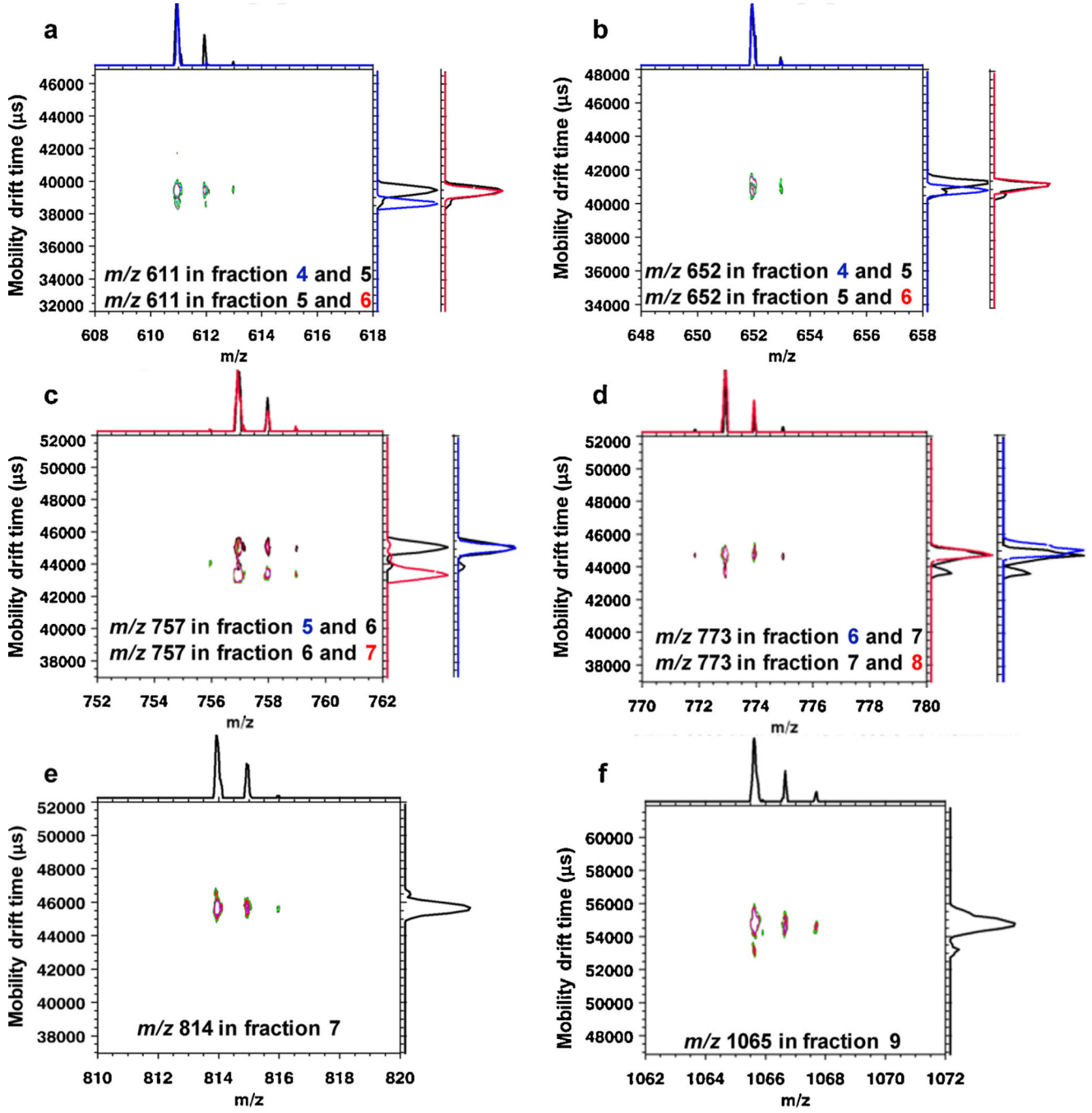


**Fig. 2.**

Evaluation of isomeric heterogeneity of oligosaccharide-alditols released from BSM by IM-TOFMS. Shown are overlaid mobility profiles for representative oligosaccharide-alditol ions having selected *m/z* values from different HPLC fractions. (a) Overlaid 2D mass-mobility spectra for *m/z* 611 from fractions 4 (blue) and 5 (black). Overlaid 1D mobility spectra for *m/z* 611 from fraction 5 (black) and 6 (red) are aligned on the right. (b) Overlaid 2D mass-mobility spectra for *m/z* 652 from fractions 4 (blue) and 5 (black). Overlaid 1D mobility spectra for *m/z* 652 from fractions 5 (black) and 6 (red) are shown on the right. (c) Overlaid 2D mass-mobility spectra for *m/z* 757 from fractions 6 (black) and 7 (red). Included on the

NIH-PA Author Manuscript

NIH-PA Author Manuscript

NIH-PA Author Manuscript

right are overlaid 1D mobility spectra for *m/z* 757 from fractions 5 (blue) and 6 (black). (d) Overlaid 2D mass-mobility spectra for *m/z* 773 from fractions 7 (black) and 8 (red). Displayed on the right are overlaid 1D mobility spectra for *m/z* 773 from fraction 6 (blue) and 7 (black). (e) 2D IMMS plot of *m/z* 814 from fraction 7; (f) 2D IMMS plot of *m/z* 1065 from fraction 9. (Note that the overlaid 1D mobility spectra share the same drift time scale with the corresponding 2D spectra). (For interpretation of the references to colour in this figure legend, the reader is referred to the web version of this article.)

NIH-PA Author Manuscript

NIH-PA Author Manuscript

NIH-PA Author Manuscript

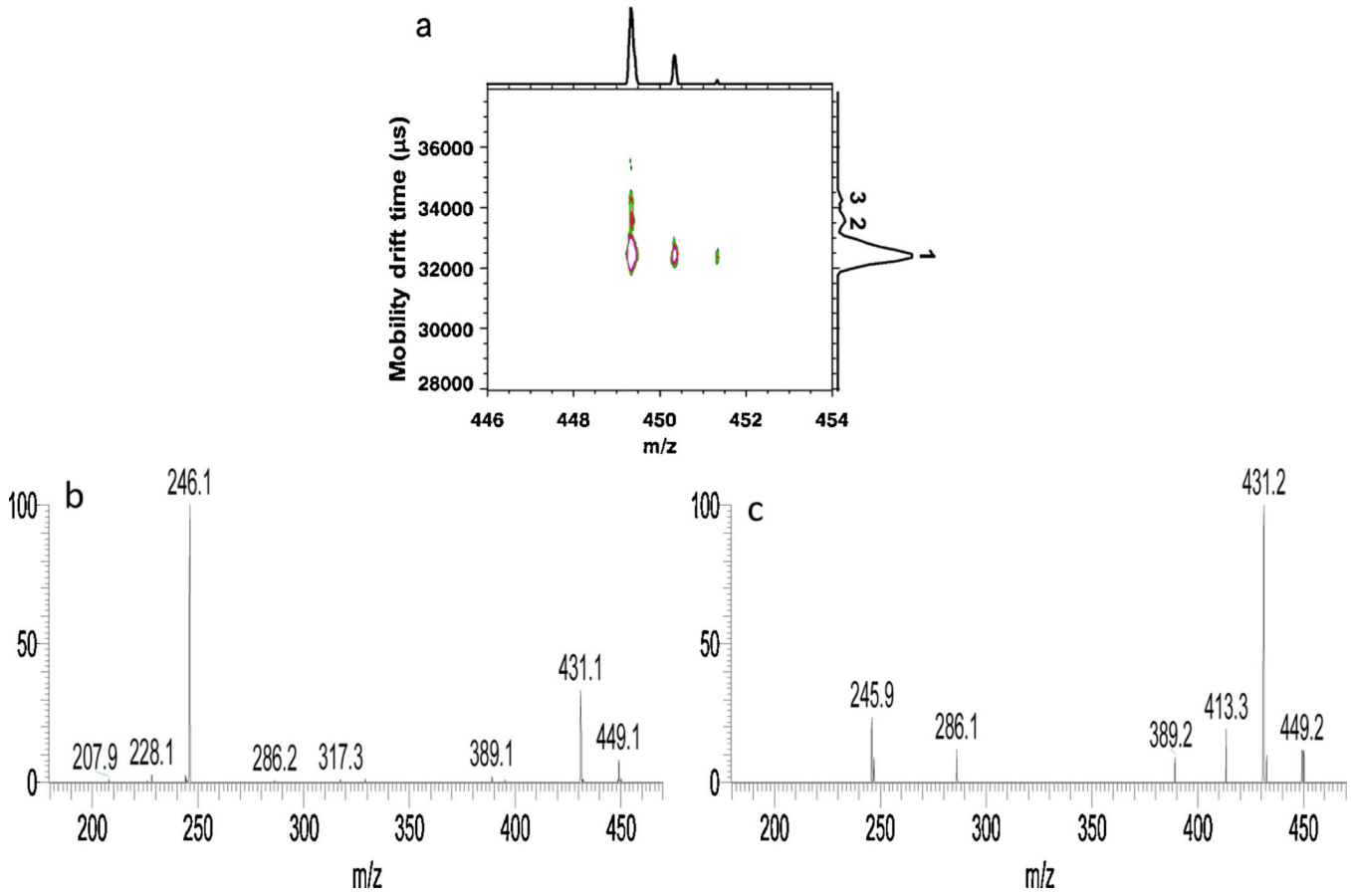


**Fig. 3.**

(a) 2D IMMS spectrum of *m/z* 449 from HPLC fraction 2 acquired on IM-TOFMS. (b) MS/MS spectrum of *m/z* 449 in LC fraction 2 from the 42.2–43.1 ms mobility window (peak 1) on the dual gate IM-QITMS. (c) MS/MS spectrum of *m/z* 449 in LC fraction 2 from the 44.1–44.6 ms (peak 2) mobility window on the dual gate IM-QITMS.

NIH-PA Author Manuscript

NIH-PA Author Manuscript

NIH-PA Author Manuscript

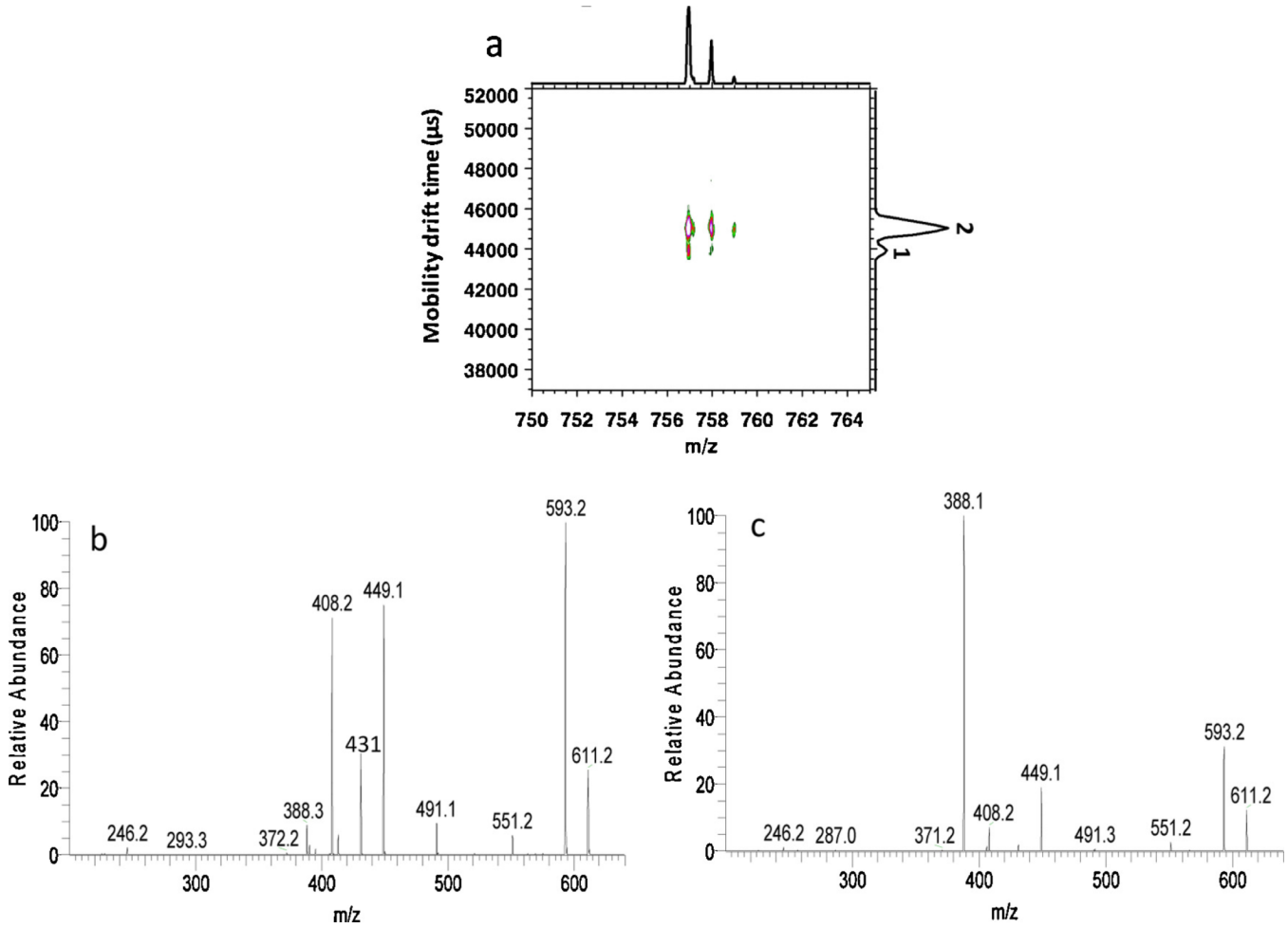


**Fig. 4.**

(a) 2D IMMS plot of *m/z* 757 from HPLC fraction 6 acquired on IM-TOFMS. (b) $MS^3$ spectrum of the *m/z* 611 product ion derived from *m/z* 757 in fraction 6 of the 57.4–58.1 ms (peak 1) mobility window on dual gate IM-QITMS. (c) $MS^3$ spectrum of the *m/z* 611 product ion derived from *m/z* 757 in fraction 6 of the 59.1–60.0 ms (peak 2) mobility window on dual gate IM-QITMS.

NIH-PA Author Manuscript
NIH-PA Author Manuscript
NIH-PA Author Manuscript



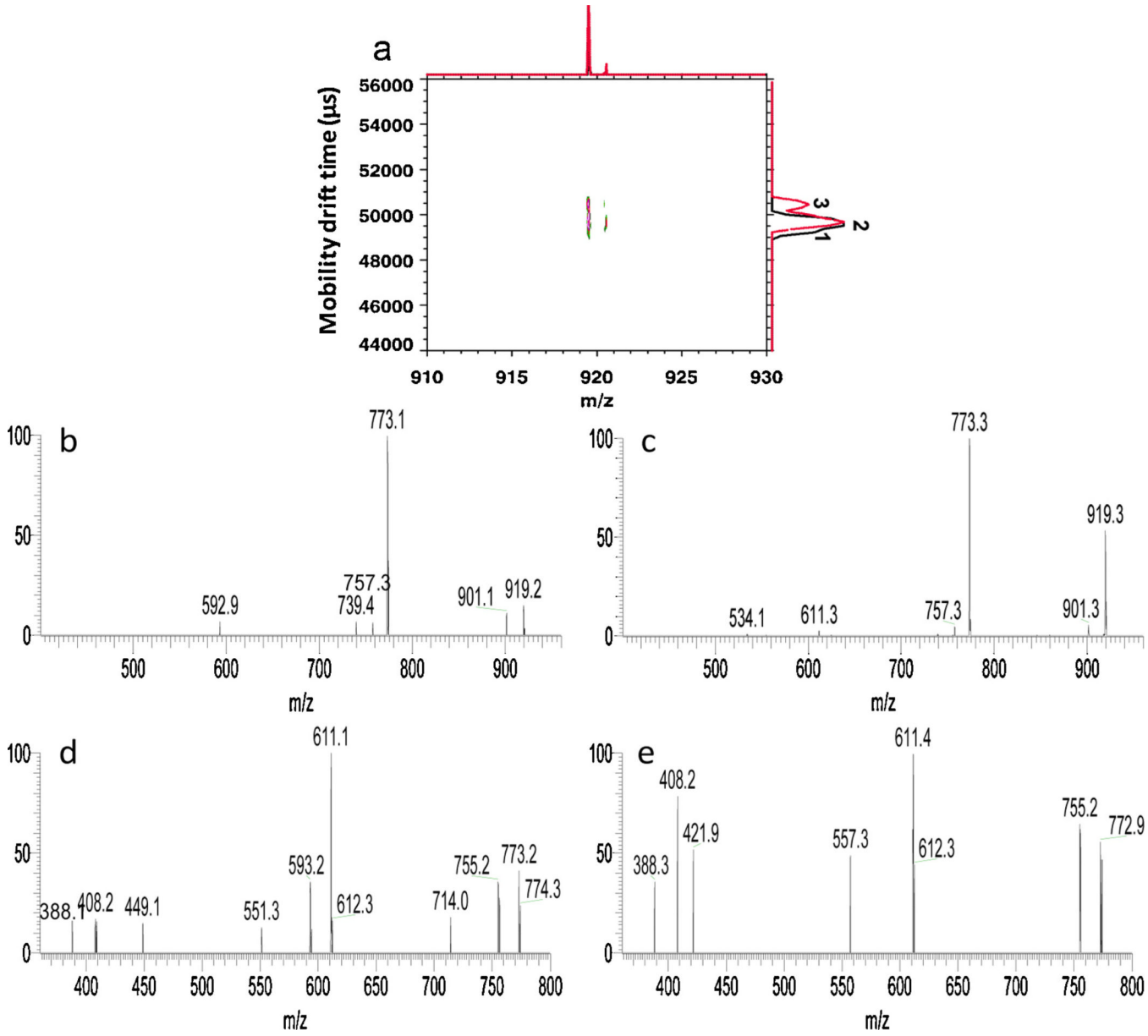


**Fig. 5.**

(a) Overlaid 2D IMMS spectra of the *m/z* 919 precursor ion from HPLC fractions 8 (black trace) and 9 (red trace) acquired on IM-TOFMS. (b) MS/MS spectrum of the *m/z* 919 precursor ion in HPLC fraction 9 of the 65.0–65.8 ms mobility window (peak 2) on the dual gate IM-QITMS. (c) MS/MS spectrum of the *m/z* 919 precursor ion in HPLC fraction 9 of the 66.4–66.9 ms (peak 3) mobility window on the dual gate IM-QITMS. (d) $MS^3$ spectrum of the *m/z* 773 product ion derived from *m/z* 919 in HPLC fraction 9 of the 65.0–65.8 ms (isomer 2) mobility window on dual gate IM-QITMS. (e) $MS^3$ spectrum of *m/z* 773 product ion derived from *m/z* 919 in LC fraction 9 of the 66.4–66.9 ms (isomer 3) mobility window on IM-QITMS. (For interpretation of the references to colour in this figure legend, the reader is referred to the web version of this article.)

NIH-PA Author Manuscript

NIH-PA Author Manuscript

NIH-PA Author Manuscript

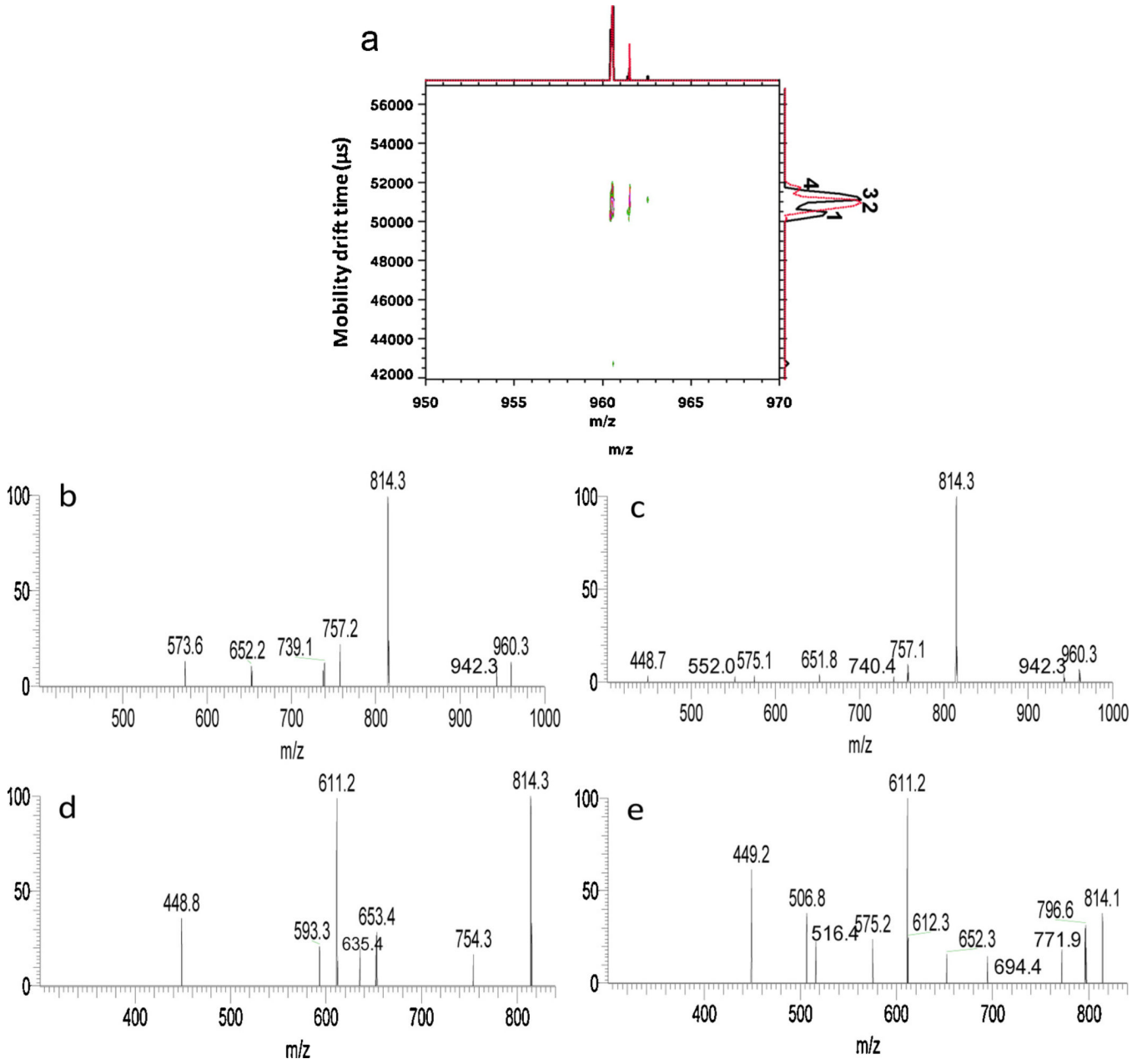


**Fig. 6.**

(a) Overlaid 2D IMMS spectra of *m/z* 960 from HPLC fractions 8 (black trace) and 9 (red trace) acquired on IM-TOFMS. (b) The MS/MS spectrum of *m/z* 960 in HPLC fraction 8 of the 66–66.6 ms (peak 1) mobility window on the dual gate IM-QITMS. (c) MS/MS spectrum of *m/z* 960 in fraction 8 of the 67.4–68.4 ms (peak 3) window on dual gate IM-QITMS. (d) $MS^3$ spectrum of the *m/z* 814 product ion derived from the *m/z* 960 precursor ion in fraction 8 of the 66–66.6 ms (peak 1) mobility window on the dual gate IM-QITMS. (e) $MS^3$ spectrum of the *m/z* 814 product ion derived from the *m/z* 960 precursor ion in fraction 8 of 67.4–68.4 ms (peak 3) mobility window on the dual gate IM-QITMS. (For interpretation of the references to colour in this figure legend, the reader is referred to the web version of this article.)